

## Persistent hole burning in multiple-scattering optical media

メタデータ	言語: eng 出版者: 公開日: 2008-02-25 キーワード (Ja): キーワード (En): 作成者: Tomita, Makoto, Ito, Tetsu, Hattori, Satoshi メールアドレス: 所属:
URL	<a href="http://hdl.handle.net/10297/592">http://hdl.handle.net/10297/592</a>

## Persistent hole burning in multiple-scattering optical media

Makoto Tomita, Tetsu Ito, and Satoshi Hattori

*Department of Physics, Faculty of Science, Shizuoka University, 836 Ohya Shizuoka 422-8529, Japan*

(Received 20 June 2001; published 22 October 2001)

We analyzed the shape and width of room-temperature persistent holes in photoreactive and multiple-scattering media in frequency and wave-vector domains. The shape and width of holes depend on sample thickness, transport mean free path, geometrical configuration, and absorption lengths. The measurements of the angular dependence of hole burning in a disordered CdS<sub>0.85</sub>Se<sub>0.15</sub>-doped glass sample were in quantitative agreement with theory.

DOI: 10.1103/PhysRevB.64.180202

PACS number(s): 42.25.Dd, 42.65.-k, 42.62.Fi

Photochemical and nonphotochemical persistent hole burning is popular in organic molecules embedded in low-temperature glassy materials.<sup>1-3</sup> When a monochromatic laser is irradiated in an inhomogeneously broadened impurity vibronic absorption band, a narrow hole with a spectral width of the order of the homogeneous linewidth is produced. The hole production is based on a site selective photobleaching process, and the mechanism is usually explained on the basis of a two-level system structure of the glassy material, which consists of asymmetric intermolecular double well potential.<sup>4</sup> The persistent hole lasts without profile change as long as the material is kept at the low temperature, and has attracted interest for its application to high-density optical data storage.<sup>5-8</sup>

Recently, a similar hole burning, but based on a totally different mechanism, has been reported in photoreactive materials combined with multiple scattering.<sup>9</sup> In a multiple-scattering medium, propagation modes exist in angular frequency domain with the mode spacing of  $\Delta\omega = 2\pi^2c^3/L^3\omega^2$ , where  $L$  is the dimension of the sample and  $c$  is the velocity of light, while each propagation mode has a spectral width of the order of inverse of photon lifetime,  $\delta\omega \sim 2\pi(D/L^2) = 2\pi(cl^*/3L^2) \equiv 2\pi\tau_{life}^{-1}$ , where  $D$  is the diffusion constant and  $l^*$  is the transport mean free path.<sup>10-13</sup> Consider a disordered medium of 1 mm thickness with the transport mean free path of 10  $\mu\text{m}$ , the spectral width could be  $\delta\omega \sim 6.3$  GHz. We see a correspondence of  $\delta\omega$  in multiple-scattering medium to the homogenous linewidth in the inhomogeneously broadened band in impurity molecules in glassy material.<sup>12,13</sup> It has also been pointed out that there is analogy between fluorescence line narrowing measurement and correlation measurements of fluctuations in disordered media. Since each propagation mode has its own complex spatial mode pattern, if one could photobleach such a spatial pattern in the medium, persistent hole could be burned in the frequency domain at room temperature.

This is reminiscent of the use of Lippman holograms, which are the basis of an optical data storage method using the interference of incident beams.<sup>14</sup> In the Lippman hologram, optical data are stored in the three-dimensional interference pattern of standing wave, whereas in multiple-scattering medium, data are stored in the three-dimensional random interference speckle pattern.<sup>15</sup> A single volume medium can, therefore, store a great many coexisting data at one time when the recording angle is changed. In this paper, we

calculated the shape and width of the persistent hole on the basis of the intensity correlation of fluctuations in multiple-scattering media. We also present a hole burning experiment in CdS<sub>0.85</sub>Se<sub>0.15</sub>-doped disordered glass<sup>16-18</sup> in order to compare theory with experiment.

The production mechanism of the hole is explained as follows. First, a recording beam with the incident frequency  $\omega_1$  and wave vector  $k_1$  is injected onto a multiple-scattering medium. The injected light propagates through the medium, producing a random interference pattern, i.e., a volume speckle. This pattern is recorded in the medium through a photobleaching process. After the pattern is recorded, the luminescence intensity from the sample excited by a reading beam of  $\omega_2$  and  $k_2$  is monitored as a function of  $\Delta\omega = \omega_2 - \omega_1$  and  $\Delta k = k_2 - k_1$ . Consider that the frequency and wave vector of the recording and reading beams coincide, the spatial fluctuation patterns produced by the two beams also coincide with respect to each other. The reading beam, then, excites only the photobleached portion of the medium, the luminescence intensity being reduced. We will observe a dip in the luminescence intensity as a function of  $\Delta\omega$  and  $\Delta k$ . The process is, therefore, described on the basis of the intensity correlation of fluctuations inside the medium. The shape of the observed hole,  $H(\Delta\omega, \Delta k)$ , may be represented as,

$$H(\Delta\omega, \Delta k) = \eta \int \int dr dr_d C(\Delta\omega, \Delta k, r) T(r, r_d), \quad (1)$$

where  $C(\Delta\omega, \Delta k, r)$  is the cumulant intensity correlation function between fluctuations produced by the recording and reading beams at  $r$  inside the medium,  $T(r, r_d)$  is the diffusive intensity propagator of the luminescence light from  $r$  to outgoing point  $r_d$ , and  $\eta$  is the efficiency of the hole production. The intensity correlation function  $C(\Delta\omega, \Delta k, r)$  is represented as,

$$\begin{aligned} C(\Delta\omega, \Delta k, r) &= \langle \delta I(\omega_1, k_1, r) \delta I(\omega_2, k_2, r) \rangle \\ &= \langle E(\omega_1, k_1, r) E^*(\omega_1, k_1, r) \\ &\quad \times E(\omega_2, k_2, r) E^*(\omega_2, k_2, r) \rangle - \langle I \rangle^2, \quad (2) \end{aligned}$$

where the angular bracket  $\langle \rangle$  represents an ensemble average over disordered configurations,  $\delta I(\omega, k, r) = I - \langle I \rangle$  and  $E(\omega, k, r)$  are the local intensity fluctuation and the electric field at  $r$  produced by the incident beam of frequency  $\omega$  and

wave vector  $k$ . Each local electric field in Eq. (2) is expressed as a sum of fields propagated along all possible trajectories in the medium,

$$C(\Delta\omega, \Delta k, r) = \left\langle \sum \sum \sum \sum_{\text{all trajectories}} \right. \\ \times W_1 \exp[-i\{\omega_1(t-s_1/c) + k_1 R_1\}] \\ \times W_2^* \exp[i\{\omega_1(t-s_2/c) - k_1 R_2\}] \\ \times W_3 \exp[-i\{\omega_2(t-s_3/c) + k_2 R_3\}] \\ \left. \times W_4^* \exp[i\{\omega_2(t-s_4/c) - k_2 R_4\}] \right\rangle - \langle I \rangle^2, \quad (3)$$

where  $P_i = |W_i|^2$  is the probability that the intensity propagates along a trajectory  $i$ ,  $R_i$  is the vector parallel to the incident surface that represents the entrance point of trajectory  $i$ , and  $s_i$  is the length of the trajectory  $i$ . The intensity correlation in the disordered medium can be expanded with a dimensionless conductance  $g = l^* N/L$ , and higher order correlations, the long and infinite range correlations, are also developed.<sup>19–23</sup> In this article, we only consider the leading order correlation and ignore the higher order correlations since they are  $g^{-1}$  and  $g^{-2}$  order of magnitude smaller. There are two types of terms in the summation of Eq. (3) for which the ensemble average does not vanish. We also replace the sum of trajectories with an integration of the distribution function of the trajectories,  $\sum |W_i|^2 \rightarrow \int \int dR ds P(R, s)$ . Eq. (1) is written as,

$$H(\Delta\omega, \Delta k) = \eta \int \int dr dr_d \left| \int \int dR ds \right. \\ \left. \times P(R, s) \exp[-i\{\Delta\omega s/c + \Delta k R\}] \right|^2 T(r, r_d). \quad (4)$$

Let us consider a slab sample with a thickness of  $L$  and an incident beam larger than  $L$  and calculate the shape and width of the hole. For simplicity, we assume that the absorption length for the recording and reading beams are the same since the frequency difference between two beams is generally small compared with the absorption band of the photo-reactive material, whereas the absorption length for the luminescence light is different owing to the large Stokes shift. The diffusive absorption lengths are denoted  $L_a = \sqrt{l^* l_a/3}$  and  $L_{al} = \sqrt{l^* l_{al}/3}$ , where  $l_a$  and  $l_{al}$  are absorption lengths without scattering for the recording and reading beams and for the luminescence light, respectively. The distribution function of the trajectories are calculated on the basis of the diffusion approximation. We take the  $z$  axis to be perpendicular to the incoming surface and the slab sample to occupy the space  $0 < z < L$ . The absorbing walls are set at  $z = -0.7l^*$  and  $z = L + 0.7l^*$ .<sup>24,25</sup> The distribution function is

$$P(R, s) = \int \int ds' dr' G_0(r-r', s-s') \delta(s') \delta(R') \\ \times \sum_n \{ \delta(z' - [2n(L + 1.4l^*) + s_0]) \\ - \delta(z' + [2n(L + 1.4l^*) + s_0 + 1.4l^*]) \}, \quad (5)$$

where  $s_0$  is the source point,  $r'^2 = R'^2 + z'^2$  and  $G_0(r, s) = \exp[-cr^2/4Ds]$  is the Green function in an infinite medium. Using Eqs. (3) and (5), we obtain,

$$C(\Delta\omega, \Delta k, z) = \frac{\cosh(2\gamma(L + 0.7l^* - z)) - \cos(2\delta(L + 0.7l^* - z))}{\cosh(2\gamma(L + 1.4l^*)) - \cos(2\delta(L + 1.4l^*))}, \quad (6)$$

where  $\gamma + \delta i = \sqrt{\Delta k^2 + (1/\tau_a + i\Delta\omega)/D}$ .<sup>10–13,21–23</sup> The propagator  $T(z, z_d)$  is also calculated on the basis of the diffusion approximation as,

$$T(z, z_d) = \frac{\sinh((z_1 + 0.7l^*)/L_{al}) \sinh((L + 0.7l^* - z_2)/L_{al})}{(1/L_{al}) \sinh((L + 1.4l^*)/L_{al})}, \quad (7)$$

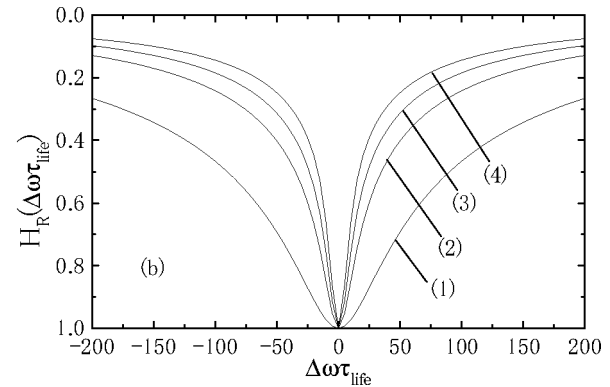
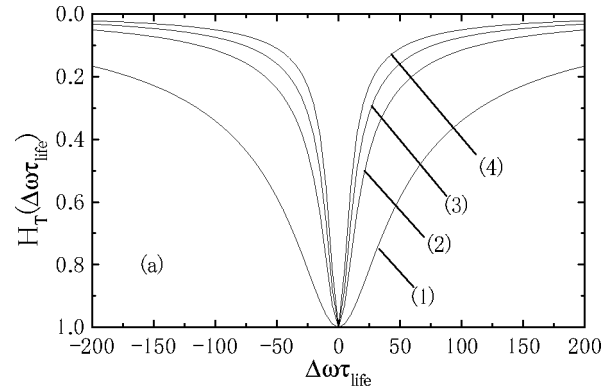


FIG. 1. Calculated curves for the hole as a function of  $\Delta\omega\tau_{life}$  for (a) transmission, and (b) reflection geometries.  $L_a$  is, (1)  $0.2L$ , (2)  $0.4L$ , (3)  $0.6L$ , and (4)  $1.4L$ .  $L_{al} = \infty$  and  $l^* = 0.033L$ . All curves are normalized.

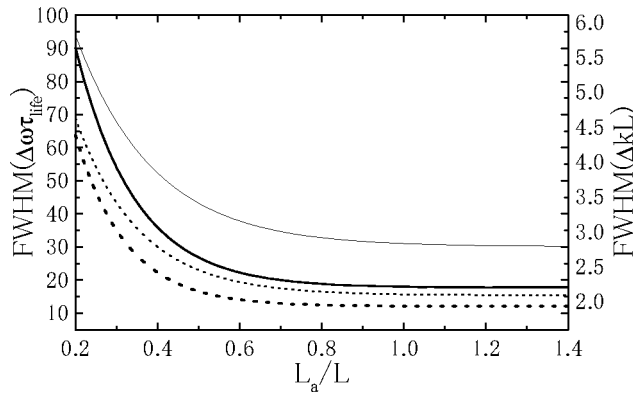


FIG. 2. The width of the hole as a function of  $L_a$ . The dotted and solid lines are for the transmission and reflection geometries, respectively. The thick and thin lines are for  $H(\Delta\omega\tau_{life})$  and  $H(\Delta kL)$ .  $L_{al}=\infty$  and  $l^*=0.033L$ .

where  $z_1=z$ ,  $z_2=z_d=L-l^*$  for the transmission geometry and  $z_1=z_d=l^*$ ,  $z_2=z$  for the reflection geometry, respectively. The shape of the hole for the transmission and reflection geometry are calculated on the basis of Eqs. (1), (6), and (7). Figure 1 shows calculated curves for the hole shape as a function of  $\Delta\omega$ , i.e.,  $H(\Delta\omega,0)$ , for different absorption lengths of the recording and reading beams,  $L_a$ . A similar calculation was also performed in  $\Delta k$  domain. The full-width at half-maximum (FWHM) of the hole are plotted in Fig. 2 as a function of  $L_a$ . The width of the hole becomes broad in all four cases shown in Figs. 1 and 2 with increasing the absorption. When  $L_a < L$ , absorption terminates long trajectories.<sup>26,27</sup> This effect broadens the intensity correlation functions  $C(\Delta\omega)$  and  $C(\Delta k)$ , and also the width of the holes in accordance with Eq. (1). In Fig. 3, we examined the dependence of the hole width on the absorption length for the luminescence,  $L_{al}$ . The parameter used are  $l^*=0.033L$  and  $L_a=0.6L$ . The hole width becomes broad in the reflection geometry, whereas the width becomes narrow in the transmission geometry when the absorption is increased. In the transmission geometry, the absorption  $L_{al}$  terminates the luminescence light coming from the small  $z$  region, where the

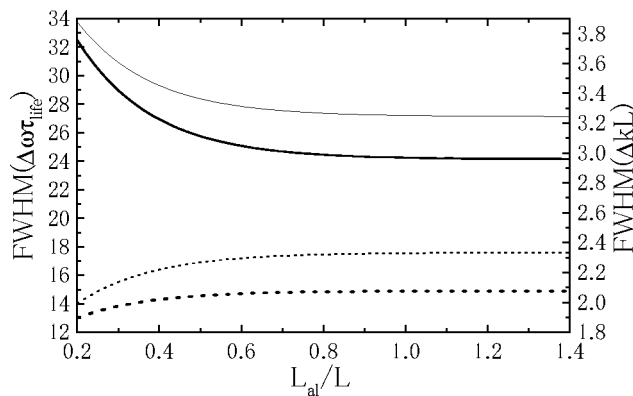


FIG. 3. The width of the hole as a function of  $L_{al}$ . The dotted and solid lines are for the transmission and reflection geometries, respectively. The thick and thin lines are for  $H(\Delta\omega\tau_{life})$  and  $H(\Delta kL)$ , respectively.  $L_a=0.6L$  and  $l^*=0.033L$ .

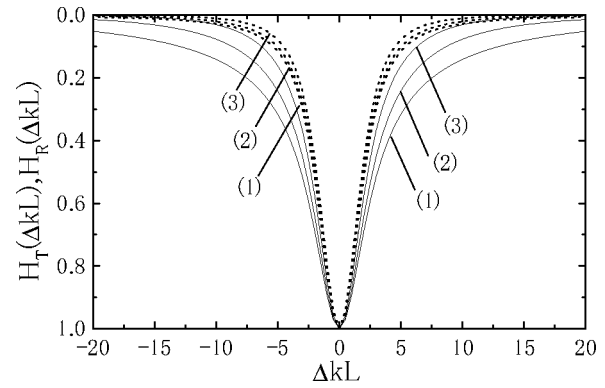


FIG. 4. Calculated curves for  $H(\Delta kL)$ .  $l^*$  is (1)  $0.01L$ , (2)  $0.03L$ , and (3)  $0.06L$ . The dotted and solid lines are for the transmission and reflection geometries, respectively.  $L_a=\infty$  and  $L_{al}=\infty$ . All curves are normalized.

mean path difference  $\Delta\xi$  is relatively small and  $C(\Delta\omega)$  and  $C(\Delta k)$  are broad. We also examined the dependence of the hole on  $l^*$ . The result is shown in Fig. 4. In the transmission geometry, the hole is almost independent of  $l^*$  as long as  $l^* \ll L$ , while in the reflection geometry, the width becomes narrow with increasing  $l^*$ . In the reflection geometry, the main contribution to the hole arises from trajectories existing in the small  $z$  region, and  $l^*$  is relevant to  $\Delta\xi$ .

We performed a hole burning experiment in a disordered  $\text{CdS}_x\text{Se}_{1-x}$ -doped glass in  $\Delta k$  domain and compared the results with the theoretical calculations.  $\text{CdS}_x\text{Se}_{1-x}$ -doped glasses are silicate glasses in which  $\text{CdS}_x\text{Se}_{1-x}$  microcrystallites of several tens to a hundred angstrom are embedded.<sup>16–18</sup> They have attracted much interest for their unique properties based on the quantum confinement and large surface effects of microcrystallites. When a laser beam is irradiated on these glasses, the luminescence intensity is fatigued whereas the absorption spectrum is kept almost intact.<sup>16,18</sup> This is referred to as photodarkening effect. The mechanism has been discussed in terms of the surface trapping state. We use this effect as the photoreactive process to record the volume speckle in the medium.

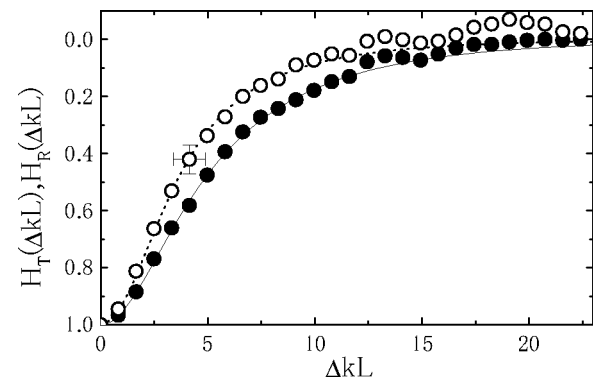


FIG. 5. Experimental results of the normalized hole as a function of  $\Delta kL$  in disordered  $\text{CdS}_{0.85}\text{Se}_{0.15}$ -doped glasses. Open and solid circles are for the transmission and reflection geometries, respectively. The dotted and solid lines are theoretically calculated curves for the transmission and reflection geometries, respectively.

The incident light source was the second harmonics of semiconductor laser pumped  $\text{Nd}^{3+}$  yttrium aluminum garnet (YAG) laser. The wavelength was 532 nm. The sample was  $\text{CdS}_{0.85}\text{Se}_{0.15}$  ( $x=0.85$ )-doped glass. The glass was grained into powder of micrometer size. This powder was compacted into a slab geometry with a thickness of 1.0 mm between two optical glass plates and used as the multiple-scattering sample. The absorption length at 532 nm was  $l_a=7.0$  mm, whereas at the luminescence wavelength of 605 nm the absorption was almost negligible. The transport mean free path was determined to be  $30 \mu\text{m}$  from a total transmission experiment. In our experiments, only one laser beam was used. First, the laser beam was irradiated on the sample for 80 s to record the volume speckle pattern through the photodarkening effect. Then the beam was attenuated in intensity and used as the reading beam to excite the luminescence. The luminescence was collected both in the transmission and reflection geometries and led into a monochromator and detected by a photomultiplier tube. The typical laser power was 400 mW for the recording beam and 2 mW for the reading beam. Note that no speckle fluctuation outside the medium was recorded in the present experiment. The sample was set

on a stage and rotated by a stepping motor to change the angle between the incident beam and the sample. The luminescence intensity as a function of  $\Delta kL$  is shown in Fig. 5. It is seen that the intensity shows a dip around  $\Delta kL \sim 0$  and the persistent hole is formed in the sample. The typical depth of the hole was 6%. The dotted and solid lines show theoretically calculated curves on the basis of Eq. (1). The parameters used are  $L_a=0.28L$ ,  $L_{al}=\infty$ , and  $l^*=0.033L$ . We see a quantitative agreement with experiment and theory. We did not take the effect of the internal reflection at the interfaces of the sample into account.<sup>28</sup> Assuming the volume fraction of the sample to be 0.74, the effective refractive index of the disordered  $\text{CdS}_x\text{Se}_{1-x}$  glass may be estimated to be 1.38, which is smaller than that of the glass plates sporting the sample, 1.52. The internal reflection at the interface is estimated to be 0.019 and may not be important in our case.

In conclusion, we analyzed the persistent holes in multiple-scattering media on the basis of the intensity correlation of fluctuations. The measurements of the angular dependence of hole burning in disordered  $\text{CdS}_{0.85}\text{Se}_{0.15}$ -doped glass sample were in quantitative agreement with theory.

- 
- <sup>1</sup>*Spectroscopy and Excitation Dynamics of Condensed Molecular Systems*, edited by V. M. Agranovich and R. M. Hochstrasser (North-Holland Publishing Company, Amsterdam, New York, 1983).
- <sup>2</sup>B.M. Kharlamov, R.I. Personov, and L.A. Bykovskaya, *Opt. Commun.* **12**, 191 (1974).
- <sup>3</sup>A.A. Gorokhovskii, R.K. Kaarli, and L.A. Rebane, *JETP Lett.* **20**, 216 (1974).
- <sup>4</sup>J.M. Hayes and G.J. Small, *Chem. Phys. Lett.* **54**, 435 (1978).
- <sup>5</sup>R. Jaaniso and H. Bill, *Europhys. Lett.* **16**, 569 (1991).
- <sup>6</sup>J. Zhang, S. Huang, and J. Yu, *Opt. Lett.* **17**, 1146 (1992).
- <sup>7</sup>M. Mitsunaga, N. Uesugi, H. Sasaki, and K. Karaki, *Opt. Lett.* **19**, 752 (1994).
- <sup>8</sup>A. Kurita, T. Kushida, T. Izumitani, and M. Matsukawa, *Opt. Lett.* **19**, 314 (1994).
- <sup>9</sup>A. Kurita, Y. Kanematsu, M. Watanabe, K. Hirata, and T. Kushida, *Phys. Rev. Lett.* **83**, 1582 (1999).
- <sup>10</sup>A.Z. Genack, *Phys. Rev. Lett.* **58**, 2043 (1987).
- <sup>11</sup>A.Z. Genack, *Europhys. Lett.* **11**, 733 (1990).
- <sup>12</sup>M. Tomita, K. Shimano, and K. Nakata, *Phys. Rev. B* **54**, R3687 (1996).
- <sup>13</sup>K. Shimano and M. Tomita, *Phys. Rev. B* **58**, 5160 (1998).
- <sup>14</sup>For example, E. Hecht, *Optics* (Addison-Wesley, Reading, Massachusetts, 1987).
- <sup>15</sup>*Laser Speckle and Related Phenomena*, edited by J.C. Dainty (Springer-Verlag, Berlin, 1984).
- <sup>16</sup>P. Roussignol, D. Ricard, J. Lukasik, and C. Flytzanis, *J. Opt. Soc. Am. B* **4**, 5 (1987).
- <sup>17</sup>M. Tomita, T. Matsumoto, and M. Matsuoka, *J. Opt. Soc. Am. B* **6**, 165 (1989).
- <sup>18</sup>M. Tomita and M. Matsuoka, *J. Opt. Soc. Am. B* **7**, 1198 (1990).
- <sup>19</sup>S. Feng, C. Kane, P.A. Lee, and A.D. Stone, *Phys. Rev. Lett.* **61**, 834 (1988).
- <sup>20</sup>W. van Haeringen and D. Lenstra, *Analogies in Optics and Micro Electronics* (Kluwer Academic Publishers, Dordrecht, 1990).
- <sup>21</sup>A.Z. Genack, N. Garcia, and W. Polkosnik, *Phys. Rev. Lett.* **65**, 2129 (1990).
- <sup>22</sup>J.F. de Boer, M.P. van Albada, and A. Lagendijk, *Phys. Rev. B* **45**, 658 (1992).
- <sup>23</sup>P. Sebbah, R. Pnini, and A.Z. Genack, *Phys. Rev. E* **62**, 7348 (2000).
- <sup>24</sup>E. Akkermans, P.E. Wolf, and R. Maynard, *Phys. Rev. Lett.* **56**, 1471 (1986).
- <sup>25</sup>*Scattering and Localization of Classical Waves in Random Media*, edited by P. Sheng (World Scientific, Singapore, 1990); *Phys. Rev. Lett.* **59**, 1420 (1987).
- <sup>26</sup>R. Berkovits, M. Kaveh, and S. Feng, *Phys. Rev. B* **40**, 737 (1989).
- <sup>27</sup>M. Tomita and T. Onimaru, *J. Phys. Soc. Jpn.* **65**, 3676 (1996).
- <sup>28</sup>J.X. Zhu, D.J. Pine, and D.A. Weitz, *Phys. Rev. A* **44**, 3948 (1991).